

Classification of brain tumor using a multistage approach based on RELM and MLBP

Mrs. R. Bhavani^{1,*} and Dr. K.Vasanth²

¹ Research Scholar, Sathyabama Institute of Science and Technology, Chennai-600119, Tamil Nadu.

² Professor/Electrical and Communication Engineering, Vidya Jyothi Institute of Technology, Hyderabad-500075, Telangana, e-mail: vasanthecek@gmail.com.

Abstract

INTRODUCTION: Automatic segmentation and classification of brain tumors help in improvement of treatment which will increase the life of the patient. Tumor may be noncancerous (benign) or cancerous (malignant). Precancerous cells may also form into cancer.

OBJECTIVES: Hough CNN is applied for selected section which applies hough casting technique in segmentation.

METHODS: A multistage method of extracting features, with multistage neighbouring is done for emerging an exact brain tumor classifying methodology.

RESULTS: In this dataset three types of brain tumors are available they are meningioma, glioma, and pituitary..

CONCLUSION: This paper presented an efficient brain tumor classification approach which involves multiscale preprocessing, multiscale feature extraction and classification.

Keywords: multistage neighbouring, modified local binary pattern, regularized extreme learning machine.

Received on 18 November 2021, accepted on 16 September 2022, published on 30 September 2022

Copyright © 2022 R. Bhavani *et al.*, licensed to EAI. This is an open access article distributed under the terms of the CC BY-NC-SA 4.0, which permits copying, redistributing, remixing, transformation, and building upon the material in any medium so long as the original work is properly cited.

doi: 10.4108/eetpht.v8i4.3082

1. Introduction

Automatic segmentation and classification of brain tumors help in improvement of treatment which will increase the life of the patient[1]. Tumor cells are collection of cells which are not in normal form, that form inflammations or developments in the body. Tumor may be noncancerous (benign) or cancerous (malignant). Precancerous cells may also form into cancer. MRI helps in imaging of the internal structure of the body. MRI utilizes magnetic fields, radio waves and computer, to capture entire image of the brain which gives more data than other techniques. It also help to find out the exact location and the size of the tumor which makes the medical practitioners to diagnose it properly. If this classification task is done manually it leads to high cost and consumes more time. There are many medical imaging methods like Computed Tomography (CT),

Single-Photon-Emission Computed Tomography (SPECT), Positron Emission Tomography (PET), Magnetic Resonance Spectroscopy (MRS), and Magnetic Resonance Imaging (MRI), which are combined to acquire the informations from the brain. In this work MRI method is preferred to obtain the details from the soft tissues[2]. Brain tumor segmentation leads to classifying the pixels which results in classification task. In this work T1 weighted contrast enhanced MRI dataset from 300 patients are taken. This dataset contains tumors such as meningiomas, gliomas, pituitary in sagittal coronal and axial views.

In brain tumor segmentation task two main approaches are adopted. One method is generative method which uses anatomical models in segmentation task. The other method is discriminative method which involves image features using expert segmentations. In paper[3] a preprocessing stage along with extraction of 70 features using combination of intensity profile, cooccurrence matrix and gabor filters. Here since skull stripping is used,

* Corresponding author. Email: bhavanipaper2021@gmail.com

it leads to difficulty in selecting the parameters, which requires more information regarding the images[5]. A comparative study of SVM and ANN analysed in paper[3]. A segmentation method using back propagation classifier [4] attains an accuracy of 95%. Fractal wavelet features [6] are given as input to SOM classifier which provides an precision of 90%. Deepneural networks help to transform feature driven problem to data driven problem[7][8][9].

A DNN model which uses both lower and higher level features by means of GPU helps to make the task faster[13]. Pyramidal multidimensional LSTM technology[14] is applied on the brain tumor segmentation which requires less number of calculation which make this task easier and speedy. Hough CNN is applied for selected section which applies hough casting technique in segmentation [15]. Leaky rectifier linear units[16] in CNN model is used in tumor segmentation. U net is used along with dice loss to handle unbalanced data[17].

A fusion between handcrafted and CNN is done in tumor segmentation[18]. Capsule network is used to overcome the drawbacks of CNN[19]. The deep features obtained from the 3D CNN remain in order to give training to the support vector machine in classifying the tumor[20]. The features are obtained using the AlexNet in CNN model for classification of tumor[21]. In cascade of LSTM and CNN in classification of tumor, VGG 16 is used in the building block of CNN, whose extracted features are applied to LSTM[22].

A daboost technique[10] along with thresholding concept is used for classifying the brain tumor. This gives an accuracy of 89.9%. Artificial neural network is applied in brain tumor as pilocytic, low ranking, anaplastic and glioblastoma multiforme[11]. A hybrid fusion of discrete cosine transform and neural network provides good accuracy in classification of tumor[12].

MRI brain tumor segmentation applying adaptively regularized kernel-based Fuzzy C-means clustering assembly[28] had the benefits of adaptability to neighborhood setting. It is also elevated with robustness to preserve image information, lack of restrictions of alignment of parameters, and reduced computational expenses. Automatic segmentation strategy depends on Convolutional Neural Networks (CNN), examining 3x3 kernels. The use of small kernels allows developing a deeper architecture other than having a constructive outcome against overfitting, giving lesser number of weights in the setup.

2. PROPOSED METHOD

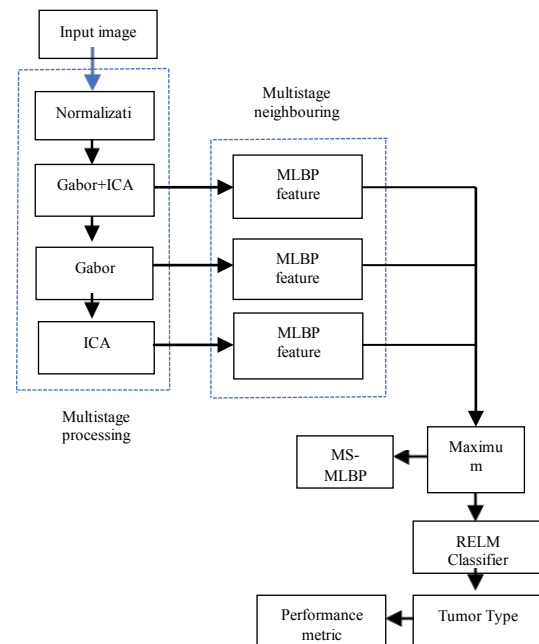


Figure 1. Block diagram of proposed method

The input brain MRI image is subjected to normalization and the normalized image underwent a multistage processing by means of gabor and ICA filters. The normalized image is subjected to gabor filter, ICA filter and hybrid combination of gabor and ICA filter. The result from each is subjected to multistage feature extraction using modified local binary pattern. In order to find the maximum value from these features maximum pooling is done and then RELM classifier is used to classify brain image into meningioma, glioma, and pituitary. Finally performance metrics are done. The detailed explanation is given below.

2.1. Normalization

Preprocessing of brain image is a significant phase which have an optimistic result on examination of brain images. The brain images, have large values beyond [0, 255], which includes nonpositive data. This phase converts the intensities of image into [0,1] by means of a min-max normalization rule

$$F(X, Y) = \frac{F(X, Y) - x_{\min}}{x_{\max} - x_{\min}} \quad (1)$$

Where F , x_{\min} and x_{\max} are the input image, least and upper extreme value in the brain image F respectively. By means of this approach, the contrast of brain boundaries and areas will be enriched and enhanced. Fig.1 shows the pre-processed result of the brain image

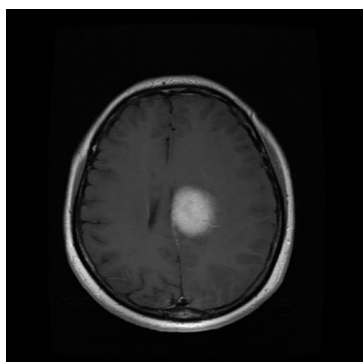


Figure 2. Pre-processed Image

2.2. Gabor texture feature extraction

The two dimensional Gabor filter[25] contains a Gaussian term controlled by frequency and orientation both in complex sinusoidal nature. It can be computed as.

$$G(X,Y) \equiv e^{-\frac{(X-X_0)^2}{2\sigma_x^2} - \frac{(Y-Y_0)^2}{2\sigma_y^2}} e^{j(\omega_x X + \omega_y Y)} \quad (2)$$

where:

ω_x, ω_y = centre frequency where better response is produced in x and y directions..

σ_x, σ_y = standard deviation in both x and y directions

X, Y = pixel location.

A total of 10 orientations are provided to the Gabor filter. Next calculate the orientation bandwidth as, $\Delta\theta = 360/8 = 45^\circ = 0.7857$ rad. The centre of the frequency ρ_i is given by

$$\rho_i = \frac{W_i + W_{i-1}}{2} = \frac{1}{2}(2^i W_0 - 2^{i-1} W_0) = 2^{i-1} \cdot 3W_0 \quad (3)$$

For an 256x256 image , 20 Gabor filters are used.

2.3 ICA filter

The image is divided into patches $p(X,Y)$ which is expressed as

$$p(X,Y) = \sum_{i=1}^N S_i A_i(X,Y) \quad (4)$$

Two terms are involved in ICA filters[23] they are mixing matrix A_a and separating matrix w_a . They are expressed as

$$A_a(X_a, Y_a) = [A_1(x_a, y_a), A_2(x_a, y_a) \dots A_N(x_a, y_a)] \quad (5)$$

$$W_a(X_a, Y_a) = [W_1(x_a, y_a), W_2(x_a, y_a) \dots W_N(x_a, y_a)] \quad (6)$$

These represent a group of filters in order to analyse the image. Here N number of filters are used for filtering the image $I(X_a, Y_a)$ to get an filtered image $Y[(I(X_a, Y_a))]$, which is defined as

$$Y[I(X_a, Y_a)] = [I(X_a, Y_a) \otimes W_1(x_a, y_a), I(X_a, Y_a) \otimes W_2(x_a, y_a) \dots I(X_a, Y_a) \otimes W_N(x_a, y_a)] \quad (7)$$

Where \otimes is convolution operator.

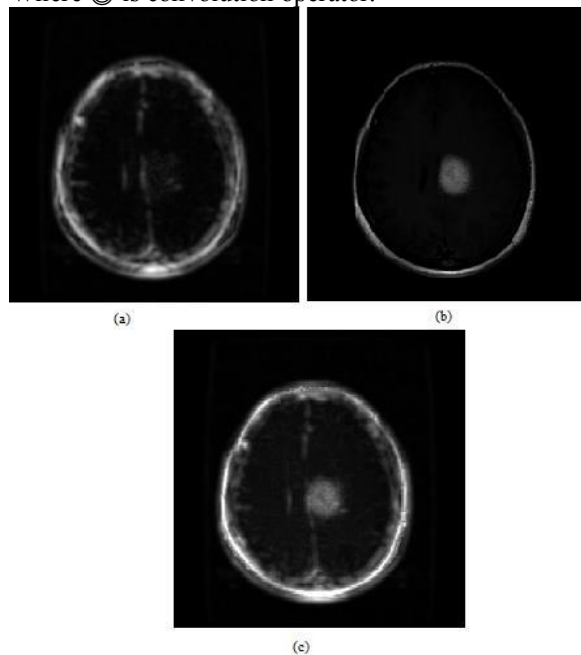


Figure 3 Multistage processing result: (a) Gabor Filter (b)ICA Filter (a) Gabor Filter (c)Gabor+ICA Filter

Steps to extract ICA filters

Step1: Consider a image set having same type of images for applying ICA filters.

Step2: The images in the set are filtered using a nonlinear filter so that high frequency component is enriched.

Step3: Select N patches from the image that satisfies the condition

$$X_m = A \cdot S_m \text{ and } Y_m = W \cdot X_m \quad (8)$$

Where A is the mixing matrix and W is the separating matrix. X_m and Y_m represent the independent sources and estimation of independent sources respectively.

Step4: By applying PCA the dimension of the matrix is reduced and n_a eigen vectors are obtained.

Step5: Apply the eigen vectors obtained in step4 to the fast ICA filters and N filters having matrix W

Image features using ICA filters

Step1: After extracting ICA filters, calculate the response of the filter using expression

$$R(X,Y) = F \otimes I(X,Y) \quad (9)$$

Step2: A map of activity is obtained which comprises the index of all active filters at each and every pixel. This is expressed as

$$A(X_a, Y_a) = \text{argmax}(R(X_a, Y_a)) \quad (10)$$

Step3: Compute the histogram of $A(X_a, Y_a)$, and find the global features of the image by scaling this histogram to interval [0 255]

Step4: Calculate how many times a filter remains in most active state in an area A using a sliding window. This provides a matrix denoted as $L(X,Y)$

Step5:To obtain the local features ,first find the histogram of L(Xa,Ya) and convert it in the range of [0 255]

2.4 Modified local binary pattern

The LBP is one of the utmost standard texture descriptors used in computer visualization and image investigation. The advantages are invariance to illumination conditions, low cost of computation, and easiness in construction. A huge amount of LBP alternatives to perform advancements in its power, robustness, and applicability is proposed. In this paper MS-MLBP descriptor is used. MLBP will encode the relationship in neighbouring region between central point and its neighbours. It has more data's which are available spatially. The MLBP [7] comprises of LBPs three in number such as the intensity value of the central pixel (E-CI), its neighboring pixels in radial directions along the radius R (E-NI), and difference between central pixel(Gc) and its local pixels in radial directions (E-RD). By applying the central pixel intensities the neighbouring intensities are calculated. The E-CI descriptor compares Gc with the mean of neighbouring pixels shown as

$$\beta = \frac{1}{n} \sum_{N=0}^{n-1} Gc \tag{11}$$

Which is given as

$$E - CI = I(Gc - \beta), I(x) = \begin{cases} 1 & \text{if } x \geq 0 \\ 0 & \text{if } x < 0 \end{cases} \tag{12}$$

E-NI represent the features extracted from the intensity vales of local pixels pl. There are pl local pixels assumed to be in a circle with radius and intensity as R and Gpr respectively. By equating the local pixels with their associated mean value which is represented as β , the E-NI descriptor translates the intensities as

$$E - NI = \sum_{N=0}^{pl-1} I(Gpr, N - \beta) 2^N \tag{13}$$

This forms a pattern, which is pl bit in binary form. This is shifted into its decimal equivalent.

E-RI encodes the intensity difference of two circles having radius R and RI. E-RI is defined as

$$E - RI = \sum_{N=0}^{pl-1} I(Gpr, N - Gpr - 1, N) 2^N \tag{14}$$

E-RI and E-NI can produce 2^N different binary pattern. In order to remove rotational effect and reduce pattern dimension rotational invariant and uniform mapping is done. The updated operators are $[(E-NI)]^{\wedge}riu2$ and $[(E-RI)]^{\wedge}riu2$ where $u2$ and ri represent the uniform mapping and rotational invariant respectively.

MLBP is inappropriate in classification of images having different scale values. The output MLBP (Pi, Ri), $i = 1, 2, \dots, N$, associate the patterns in MLBP (Pi, Ri), first concatenate the patterns using joint histogram then calculate the corresponding histogram. This shows the conversion of multidimensional to one dimensional

histogram. The joint histograms of E-CI, E-RI and E-NI are denoted as $[(E-CI/NI/RI)]_{(i)}^{\wedge}(ri,u2)$.

The MS-ELBP is calculated as $E - CI/NI/RI_{i(i)}^{riu2}$

$$\text{where } l(i) = \sum_{i=1}^N (Pi, Ri) \tag{15}$$

An image is partitioned into 20 cells with size $2*8$, then by various threshold values for local circles and radius such as (pl = 10, R = 2), (pl = 14, R = 3.5) and (pl = 17, R = 5). The extracted features compares the center pixel with surrounding pixels and change the decimal value to its binary along with weighted values.

2.5 Extreme Pooling

The extreme pooling scheme is done to obtain the greatest value from the similar bins of the multi-level MLBP histogram features. For every level , the same (Pi, Ri) set is used to compute its equivalent MLBP histogram features. It is expressed as

$$H_{E-CI,RI,NI,l(i)} = MAX (E - CI/NI/RI_{i(i)}^{riu2}) \tag{16}$$

where $i=1 \dots N$

These MS-MLBP histogram features are distinguished by applying to MLBP classifier to obtain the trained models.

2.6 Regularized Extreme Learning Machine

The finishing phase of the projected methodology is classification of brain tumor, which help to categorize the brain tumor through RELM classifier. RELM [24] is a type of feedforward neural networks, which has three main layers such as input, output, and hidden layer. Initialization of weights and biases is done in a random manner for input layer, before computation of output layer weights. RELM trains the features extracted and using these features, it classify the brain tumor in an accurate procedure.

Algorithm 1

Step 1: Assign the input parameters, training , dataset used for testing whose features are been extracted and labels used for training.

Step2: Initialise the weights and biases.

Step3: Weight and biases are selected in a random manner for input layer.

Step4: Perform matrix calculation

Step5: Hidden layers are computed using equation()

$$\begin{bmatrix} g(W1.X1 + B1) & \dots & g(Wm.X1 + Bm) \\ \vdots & & \vdots \\ g(W1.Xn + B1) & \dots & g(Wm.Xn + Bm) \end{bmatrix} \text{ which is of size } n * m \tag{17}$$

where W and B are weight and bias respectively.

Step6:The weight(β) and target matrix(t) are computed by using

$$\beta = \begin{bmatrix} \beta_1^t \\ \vdots \\ \beta_m^t \end{bmatrix} \quad (18)$$

$$t = \begin{bmatrix} T_1^t \\ \vdots \\ T_n^t \end{bmatrix} \quad (19)$$

Step 7: Testing phase is performed by matrix calculation
 Step8:After calculating hidden layers ,output weights are computed as

$$\hat{\beta} = \frac{1}{(h^t h + \infty)} h^t t \quad (20)$$

Step9: Output matrix is calculated as

$$o_j = \hat{h} \hat{\beta} \quad (21)$$

Step10:Finally the testing class labels are calculated as

$$l_j = \underset{L}{\operatorname{argmax}}(o_j) \text{ where } j \in L \text{ where } L \text{ is the number of classes.} \quad (22)$$

3. RESULT AND DISCUSSION

The dataset [26,27],consist of 3070 MRI imagesof brain having tumor. The images are taken from 250 patients in transverse, lateral and frontal plane. These images are categorized to have 990,1035, 1050 axial images, sagittal images, and coronal images respectively. In this dataset three types of brain tumors are available they are meningioma, glioma, and pituitary. The size of each and every image is 512 x 512 pixels. The whole dataset is divided into four, in which only one is applied for testing and the other three are in training phase.

The parameter values are initialised as

- 1.The number of Hidden Nodes is taken as 1000, 1500, 1800 ,2000,3000 etc.
2. RELM grid search has a size as 21
- 3.The regularization parameter is taken as $(\lambda) = e(val)$, where $val \in \{-10, -9.8, -9.6, \dots, 9.8, 10\}$
- 4.The activation function is a tan function,

$$\tanh(x) = \frac{2}{1 + \exp(-2x)} - 1$$

In this approach, the brain tumor is classified as meningioma, glioma, and pituitary by varying the number of hidden layers. The projected technique is equated with traditional methods like CNN and ANN in Table 1. Fig 2 shows the chart pictorially representing Table 1. Fig 3 shows how the activation function varies with the value of x.

Table 1. Comparison of proposed method with existing methods

Type of tumor	Metrics	ANN	CNN	RELM
Meningiom a	JAC	0.5259 9	0.0531 5	0.6546 6
	HC	5.3031	10.395 6	6.9382
	Accuracy	0.9397 2	0.6073 8	0.9790 9
	Sensitivit y	1	0.6823 7	0.9475 4
	Specificit y	0.6459 9	0.1973 7	0.6415 3
Glioma	JAC	0.6559 9	0.0541 5	0.6746 6
	HC	5.2031	10.195 6	6.9482
	Accuracy	0.9597 2	0.6053 8	0.9690 9
	Sensitivit y	1	0.6623 7	0.9275 4
	Specificit y	0.6359 9	0.1863 7	0.6515 3
Pituitary	JAC	0.6259 9	0.0631 5	0.6346 6
	HC	6.4031	10.295 6	6.9282
	Accuracy	0.9497 2	0.6083 8	0.9890 9
	Sensitivit y	1	0.6723 7	0.9375 4
	Specificit y	0.6259 9	0.1963 7	0.6515 3

Table 2. Performance metrics by varying the number of hidden layers

Number of hidden layers	Accuracy	Sensitivity	Specificity	Precision	F1-Score
1000	0.9585	0.9584	0.9745	0.9999	0.978
1500	0.9614	0.9612	0.9831	0.9999	0.9802
1800	0.9675	0.9686	0.8986	0.9986	0.9834
2000	0.9770	0.9785	0.8534	0.9983	0.9883
3000	0.9712	0.9656	0.9900	0.9999	0.9888

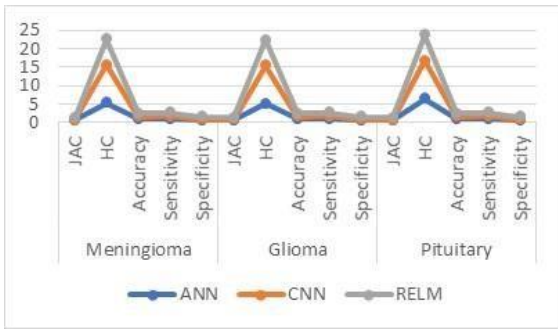


Figure 4. Performance metrics of various methods compared with existing methods

Table 2 shows that the proposed method is analysed by varying the number of hidden layers. It is observed that the 2000 layers provide greater accuracy than other layers. Fig 4 represents graphical variation of proposed method in various number of hidden layers.

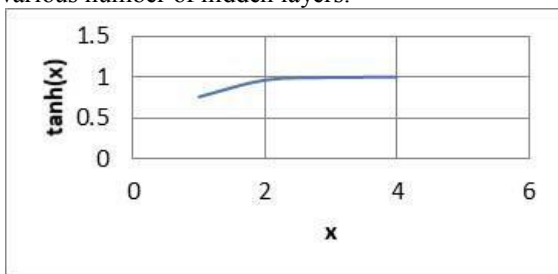


Figure 5. The variation of activation function for value of x

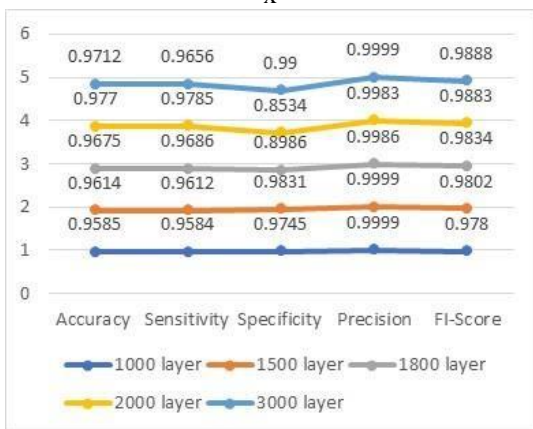


Figure 6. Performance metrics by varying the number of hidden layers

Table 3. Performance of proposed method by varying regularization parameter

λ	Accurac y	Sensitivit y	Specificit y	Precisio n	FI-Score
EXP(-10)	0.9385	0.9784	0.9645	0.9879	0.9828
EXP(-9.8)	0.9414	0.9812	0.9781	0.9899	0.9872

EXP(-9.6)	0.9575	0.9586	0.8826	0.9836	0.9734
EXP(9.6)	0.9670	0.9485	0.8434	0.9853	0.9783
EXP(10)	0.9812	0.9556	0.9800	0.9869	0.9788

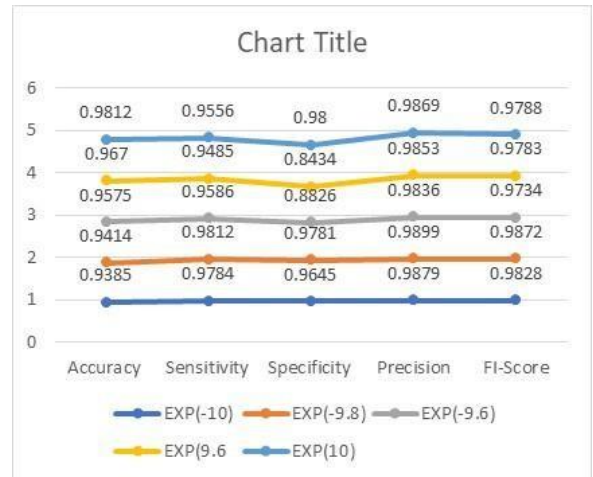


Figure 7. Performance chart by variation in regularization parameter

Table 4 explains the performance by varying the regularization parameter and its graphical plot is shown in Fig 5.

4. CONCLUSION:

This paper presented an efficient brain tumor classification approach which involves multiscale preprocessing, multiscale feature extraction and classification. At first, brain images are normalized and provided to multiscale processing. In multiscale processing the image is subjected to gabor filter, ICA filter and hybrid combination of gabor and ICA filter. The features are extracted from a multistage feature extraction technique which involves modified local binary pattern. The extracted features are applied to maximum pooling and then applied to the RELM classifier. The RELM classifier classifies into meningioma, glioma, and pituitary. The performance metric is compared with few state to art techniques like ANN and CNN. The proposed method provides an accuracy which is higher than existing techniques.

Acknowledgements

The Author with a deep sense of gratitude would thank the supervisor for his guidance and constant support rendered during this research.

References

- [1] Mohan G, Subashin, M. MRI based medical image analysis: Survey on brain tumor grade classification. *Biomed. Signal Processing Control*. 2018; 39: 139–161.
- [2] Işın A, Direkoğlu, C. Şah, M. Review of MRI-based brain tumor image segmentation using deep learning methods. *Procedia Computer Science*. 2016; 102: 317–324.
- [3] Sachdeva J, Kumar V, Gupta I, Khandelwal N, Ahuja, C.K. A package-SFERCB-“Segmentation, features extraction, reduction and classification analysis by both SVM and ANN for brain tumors”. *Applied Soft Computing*. 2016; 47: 151–167.
- [4] Sharma Y, Chhabra M. An improved automatic brain tumor detection system. *International Journal of Advanced Research in Computer Science and Software Engineering*. 2015; 5(4): 11–15.
- [5] Chaddad A, Tanougast C. Quantitative evaluation of robust skull stripping and tumor detection applied to axial MR images. *Brain Information*. 2016; 3: 53–61.
- [6] Iftekhharuddin K.M, Zheng J, Islam M.A, Ogg R.J. Fractal-based brain tumor detection in multimodal MRI. *Applied Mathematics and Computation*. 2009; 207: 23–41.
- [7] Litjens G, Kooi T, Bejnordi B.E, Arindra A, Setio A, Ciompi F, Ghafoorian M, van der Laak, J.A.W.M, van Ginneken B, Sánchez C.I. A survey on deep learning in medical image analysis. *Medical Image Analysis*. 2017; 42: 60–88.
- [8] Shelhamer E, Long J, Darrell T. Fully Convolutional networks for semantic segmentation. *IEEE Transaction Pattern Analysis Machine Intelligence*. 2017; 39: 640–651.
- [9] Badrinarayanan V, Kendall A, Cipolla R. SegNet: A deep convolutional encoder-decoder architecture for image segmentation. *IEEE Transaction Pattern Analysis Machine Intelligence*. 2017; 39: 2481–2495.
- [10] Astina M. “MR Image classification using adaboostfor brain tumor type”. *Proceeding of the 2017 IEEE 7th International Advance Computing Conference (IACC)*. 5-7 January; Hyderabad. 2017; p.p 701-705.
- [11] Jain S. Brain cancer classification using GLCM based feature extraction in artificial neural network. *International Journal of Computer Science & Engineering Technology*. 2013;4(7):966-70.
- [12] Sridhar D, Krishna IM. Brain tumor classification using discrete cosine transform and probabilistic neural network. *Proceeding of the 2013 International Conference on Signal Processing, Image Processing & Pattern Recognition*. 7-8 February; Coimbatore, India. 2013; pp. 92-96.
- [13] Havaei M, Davy A, Warde-Farley D, Biard A, Courville A, Bengio Y, Pal C, Jodoin PM, Larochelle H. Brain tumor segmentation with deep neural networks. *Medical image analysis*. 2017; 35: 18-31.
- [14] Stollenga MF, Byeon W, Liwicki M, Schmidhuber J. Parallel multi-dimensional LSTM, with application to fast biomedical volumetric image segmentation. *Advances in neural information processing systems*. 2015; 28: 2998-3006.
- [15] Milletari F, Ahmadi SA, Kroll C, Plate A, Rozanski V, Maiostre J, Levin J, Dietrich O, Ertl-Wagner B, Bötzel K, Navab N. Hough-CNN: deep learning for segmentation of deep brain regions in MRI and ultrasound. *Computer Vision and Image Understanding*. 2017; 164: 92-102.
- [16] Pereira S, Pinto A, Alves V, Silva CA. Deep convolutional neural networks for the segmentation of gliomas in multi-sequence MRI. *InBrainLes*. 2015; pp. 131-143.
- [17] Isensee F, Kickingereder P, Wick W, Bendszus M, Maier-Hein KH. Brain tumor segmentation and radiomics survival prediction: Contribution to the brats 2017 challenge. *In International MICCAI Brainlesion Workshop*. 2017; pp. 287-297.
- [18] Saba T, Mohamed AS, El-Affendi M, Amin J, Sharif M. Brain tumor detection using fusion of hand crafted and deep learning features. *Cognitive Systems Research*. 2020; 59: 221-30.
- [19] Afshar P, Plataniotis KN, Mohammadi A. Capsule networks for brain tumor classification based on MRI images and coarse tumor boundaries. *Proceeding of the ICASSP 2019-2019 IEEE International Conference on Acoustics, Speech and Signal Processing (ICASSP)*. 12-17 May; Brighton, UK. 2019; pp. 1368-1372.
- [20] Nie D, Zhang H, Adeli E, Liu L, Shen D. 3D deep learning for multi-modal imaging-guided survival time prediction of brain tumor patients. *Proceeding of the International conference on medical image computing and computer-assisted intervention*. 17 October; 2016; pp. 212-220.
- [21] Y. Xu, Z. Jia, Y. Ai, F. Zhang, M. Lai, I. Eric, and C. Chang. Deep convolutional activation features for large scale brain tumor histopathology image classification and segmentation. *Proceeding of the 2015 IEEE*
- [22] Shahzadi I, Tang TB, Meriadeau F, Quyyum A. CNN-LSTM: Cascaded framework for brain Tumour classification. *Proceeding of the 2018 IEEE-EMBS Conference on Biomedical Engineering and Sciences (IECBES)*. 3 December; Sarawak, Malaysia. 2018; pp. 633-637.
- [23] Huang B, Li J, Hu S. Texture feature extraction using ICA filters. *In2008 7th World Congress on Intelligent Control and Automation*. 25-27 June; Chongqing, China. 2008; pp. 7631-7634.
- [24] Gumaeci A, Hassan MM, Hassan MR, Alelaiwi A, Fortino G. A hybrid feature extraction method with regularized extreme learning machine for brain tumor classification. *IEEE Access*. 2019; 7: pp. 36266-36273.
- [25] Roslan R, Jamil N. Texture feature extraction using 2-D Gabor Filters. *Proceeding of the 2012 International Symposium on Computer Applications and Industrial Electronics (ISCAIE)*. 3-4 December; Kota Kinabalu, Malaysia. 2012; pp. 173-178.
- [26] Elazab A, Wang C, Jia F, Wu J, Li G, Hu Q. Segmentation of brain tissues from magnetic resonance images using adaptively regularized kernel-based fuzzy-means clustering. *Computational and mathematical methods in medicine*. 2015; 2015.medicine. 2015; 2015.
- [27] Castro, MP.; Ojeda Sánchez, JC.; Ochoa Aucay, JE. The role of intestine as a target with a therapeutic role in people with a neurodegenerative diseases. *Salud, Ciencia y Tecnología*. 2023, 3:310. <https://doi.org/10.56294/saludcyt2023310>